

## Field emission from single-crystalline HfC nanowires

Jinshi Yuan, Han Zhang, Jie Tang, Norio Shinya, Kiyomi Nakajima et al.

Citation: *Appl. Phys. Lett.* **100**, 113111 (2012); doi: 10.1063/1.3694047

View online: <http://dx.doi.org/10.1063/1.3694047>

View Table of Contents: <http://apl.aip.org/resource/1/APPLAB/v100/i11>

Published by the [American Institute of Physics](#).

---

### Related Articles

Explicit all-atom modeling of realistically sized ligand-capped nanocrystals  
*J. Chem. Phys.* **136**, 114702 (2012)

Magnetoplasmonic nanostructures based on nickel inverse opal slabs  
*J. Appl. Phys.* **111**, 07A948 (2012)

Interfacial stabilization of bilayered nanolaminates by asymmetric block copolymers  
*Appl. Phys. Lett.* **100**, 101602 (2012)

Size effect of Fe nanoparticles on the high-frequency dynamics of highly dense self-organized assemblies  
*J. Appl. Phys.* **111**, 07B517 (2012)

Self-assembly of Fe nanocluster arrays on templated surfaces  
*J. Appl. Phys.* **111**, 07B515 (2012)

---

### Additional information on *Appl. Phys. Lett.*

Journal Homepage: <http://apl.aip.org/>

Journal Information: [http://apl.aip.org/about/about\\_the\\_journal](http://apl.aip.org/about/about_the_journal)

Top downloads: [http://apl.aip.org/features/most\\_downloaded](http://apl.aip.org/features/most_downloaded)

Information for Authors: <http://apl.aip.org/authors>

## ADVERTISEMENT



**HAVE YOU HEARD?**

Employers hiring scientists  
and engineers trust  
**physicstoday JOBS**



<http://careers.physicstoday.org/post.cfm>

## Field emission from single-crystalline HfC nanowires

Jinshi Yuan,<sup>1,2</sup> Han Zhang,<sup>3</sup> Jie Tang,<sup>1,2</sup> Norio Shinya,<sup>1</sup> Kiyomi Nakajima,<sup>1</sup> and Lu-Chang Qin<sup>4,a)</sup>

<sup>1</sup>National Institute for Materials Science, Tsukuba, Ibaraki 305-0047, Japan

<sup>2</sup>Graduate School of Pure and Applied Sciences, University of Tsukuba, Tsukuba, Ibaraki 305-8577, Japan

<sup>3</sup>International Center for Young Scientist, National Institute for Materials Science, Tsukuba, Ibaraki 305-0047, Japan

<sup>4</sup>Department of Physics and Astronomy, University of North Carolina at Chapel Hill, Chapel Hill, North Carolina 27599-3255, USA

(Received 17 November 2011; accepted 14 February 2012; published online 16 March 2012)

Single HfC nanowire field emitter/electrode structures have been fabricated using nano-assembling and electron beam induced deposition. Field ion microscopy has been applied to study the atomic arrangement of facets formed on a field evaporation-modified HfC nanowire tip. Field evaporation and crystal form studies suggest that the {111} and {110} crystal planes have lower work functions, while the {100}, {210}, and {311} planes have higher work functions. Field emission measurement permits us to obtain that the work function of the {111} crystal plane is about 3.4 eV.

© 2012 American Institute of Physics. [<http://dx.doi.org/10.1063/1.3694047>]

Hafnium carbide (HfC) as a most refractory material exhibits appealing physical and chemical properties, including low electrical resistivity, low work function, high mechanical strength, high chemical stability, high wear resistance, and extremely high melting temperature of 3900 °C.<sup>1–3</sup> The brightness of an HfC electric field-induced electron emitter can be one order of magnitude higher than tungsten (W) emitter, while the energy spread of the emitted electron beam is 50% lower mainly because of its lower work function of 3.3 eV compared to W, which has a work function of around 4.5 eV.<sup>3</sup> The emission stability is also expected to improve due to its high hardness and low surface mobility which can reduce the impact of adsorption of residual molecules and ion bombardment.<sup>4</sup> Single-crystalline nanowires as well as carbon nanotubes possess a unique combination of excellent crystallinity and ideal geometry of nano-metric sharpness and uniform axial thickness. These structural characteristics make them highly feasible as candidates of high performance point electron emitters as demonstrated experimentally using rare-earth hexaboride single nanowires and single carbon nanotubes in our previous work.<sup>5–12</sup> Therefore, an HfC nanowire emitter can potentially provide a more predictable and stable performance as compared to its counterparts with cone-shaped geometry. In addition, it is possible to use a single-crystalline nanowire to obtain a clean and stable apical surface in a repeatable manner through field evaporation without applying heating (thermal flashing). The operational conditions involving thermal flashing are usually very difficult to control to obtain repeatable field emission patterns in practice.<sup>12–14</sup>

In this work, we report a study of the structure and electric field-induced electron emission of individual HfC nanowires. To study the field emission properties of a single HfC nanowire, we have assembled a single nanowire field emitter structure. Field ion microscopy (FIM) and field emission mi-

croscopy (FEM) are used to characterize the topological geometry of the tip surface to sub-nanometer precision. The FIM and FEM data combined with measurement of field emission current also enabled us to obtain the work functions of a single HfC nanowire.

HfC nanowires were synthesized using hafnium tetrachloride (HfCl<sub>4</sub>) and methane (CH<sub>4</sub>) by chemical vapor deposition (CVD) with nickel (Ni) metal as catalyst. The nanowires grew in the [001] direction and were of 20–80 nm in thickness and a few tens of microns in length. The growth of the HfC nanowires is identified to follow the vapor-liquid-solid (VLS) mechanism.

To make a field electron emitter, we picked up a single HfC nanowire and mounted it onto the tip of a W needle using a home-built nano-assembly system.<sup>12</sup> The structure of such a nanowire emitter is shown in Figure 1(a). The tip of the HfC nanowire was first modified by a field evaporation process to smoothen out the corners and edges. The process was monitored *in situ* using an FIM.<sup>15</sup> An FIM image of the HfC nanowire tip, which is composed of images recorded at 3 different exposure times to reveal more clearly the inner and outer facets, is shown in Figure 1(b). In the FIM image, facets with Miller indices of {100}, {110}, {111}, {311}, and {210} are all resolved as circular planes surrounded by concentric rings corresponding to the atomic terraces. The size of a circular plane corresponds to the area of the facet formed on the surface of the nanowire tip, which follows the order of {111} > {110} > {100} for the low index facets. This order agrees with the planar atomic packing density of the HfC crystal, which is of the NaCl-type in crystal structure with lattice parameter  $a = 0.4458$  nm. In the FIM image, the imaging atoms are Hf atoms, because C atoms are more negatively charged than Hf in the crystal.<sup>16,17</sup> Figure 1(c) is a scanning electron microscope (SEM) image of the same nanowire taken after tip-modification by field evaporation. The radius of curvature can be calculated from the FIM image using the ring counting method<sup>18</sup>

$$r = nd/(1 - \cos \theta), \quad (1)$$

<sup>a)</sup>Author to whom correspondence should be addressed. Electronic mail: lcqin@physics.unc.edu.

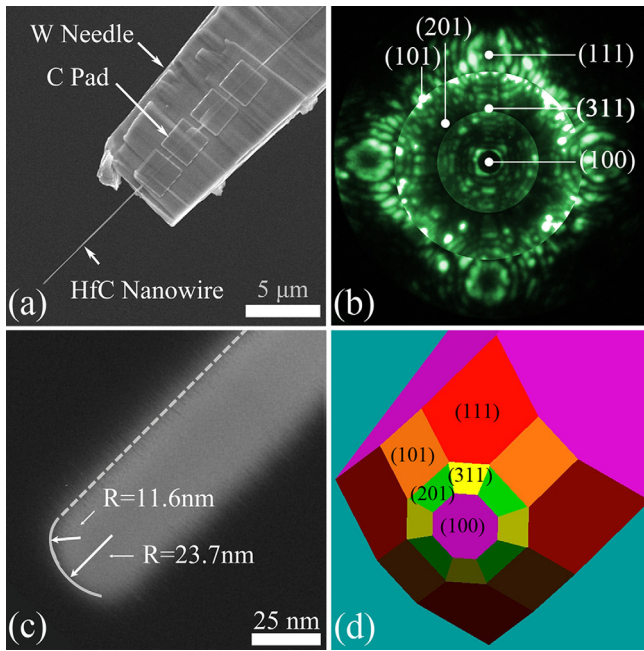


FIG. 1. (Color online) (a) SEM image of a single HfC nanowire emitter fabricated by nano-assembly and electron beam deposition. (b) FIM image from the clean surface of a  $\langle 100 \rangle$  oriented HfC nanowire tip after field evaporation. (c) SEM image of the nanowire emitter tip after field evaporation, showing rounded emission tip. (d) Reconstructed surface of the nanowire tip showing the distribution of facets of different lattice planes.

where  $r$  is the local radius of curvature,  $n$  is the number of rings between the center of one facet to the center of the adjacent facet,  $d$  is the inter-planar distance of the ring terrace, and  $\theta$  is the angle between the crystallographic directions normal to the two facets, respectively. The local radii of curvature for the  $\{100\}$  facet and the  $\{111\}$  facet were calculated to be 20.5 nm and 10.3 nm, respectively. The radii of curvature at the tip apex and the tip corner were measured

from the SEM image to be 23.7 nm and 11.6 nm, respectively, which agree well with the ring counting results. Figure 1(d) is a reconstructed model of the nanowire tip showing the distribution of facets of different lattice planes. The tip geometry remained the same even after performing field evaporation for more than 3 h at a depletion rate of one lattice plane every 30 s. It was also observed that, during raising the extraction voltage, all the facets in the image started evaporation at about the same threshold voltage. Since the radius of curvature of the outer facets is smaller than that of the inner facets, the threshold electric field for field evaporation must be higher for the outer facets than that for the inner facets under the same extraction voltage. The field evaporation threshold  $F_0$  can be obtained by considering a direct ionic evaporation over an electric field reduced energy barrier<sup>18</sup>

$$F_0 = (\Lambda + V_I - \phi)/q^3, \quad (2)$$

where  $\Lambda$  is the vaporization energy,  $V_I$  is the ionization energy,  $\phi$  is the work function, and  $q$  is the charge of the ion of interest. In the case of the HfC nanowire tip, taken  $\Lambda$  and  $V_I$  the same for all facets, the difference in  $F_0$  must come from the variation of the work function of the various surface planes. We, therefore, have observed that the  $\{111\}$  and  $\{110\}$  crystal surfaces have lower work functions than the  $\{100\}$ ,  $\{311\}$ , and  $\{210\}$  crystal surfaces. Our observation supports the conclusion that, for a compound material, the crystal planes with a higher atomic density have a lower work function whereas for an elemental material, planes with a lower atomic density have a lower work function.<sup>19</sup> We should note that our result is contrary to a previous study carried out on an electrochemically polished HfC emitter under thermal flashing, where it was reported that the work function of the  $\{111\}$  and  $\{100\}$  planes is higher.<sup>20</sup> We attribute the difference to the flatness and cleanliness of the surface being measured.

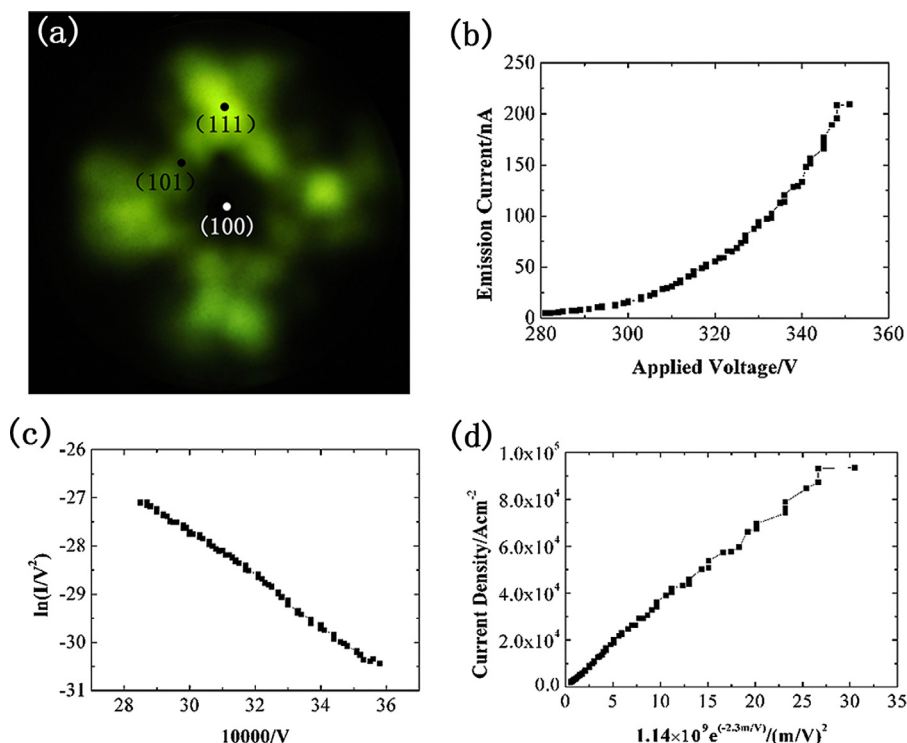


FIG. 2. (Color online) (a) Field emission pattern from the HfC nanowire. Four-fold symmetry is present in the emission pattern due to the symmetrical structure of the HfC surface. (b) Dependence of the field emission total current on extraction voltage ( $I$ - $V$  curve). (c) F-N plot obtained from (b). (d) Current density  $J$  vs.  $1.14 \times 10^9 e^{-2.3m/V}/(m/V)^2$  for deduction of work function.

After the HfC nanowire tip had been cleaned, field-induced electron emission was obtained after the extraction voltage polarity was reversed. A field emission pattern is displayed in Figure 2(a). It was observed that only the regions corresponding to the {111} planes are bright.

A typical relationship between the emission current  $I$  and the applied extraction voltage  $V$  ( $I$ - $V$  curve) from a field-evaporated clean tip is given in Figure 2(b). It was observed that  $I$  increased exponentially with respect to  $V$ . The electron emission current density  $J$  (in  $\text{A}/\text{cm}^2$ ) can be expressed by the room temperature Fowler-Nordheim equation as<sup>21</sup>

$$J = 1.54 \times 10^{-6} \frac{F^2}{\phi} \exp\left(-6.3 \times 10^9 \frac{\phi^{3/2}}{F}\right), \quad (3)$$

where  $F$  is the extraction electric field and  $\phi$  is the work function of the emission site. Replacing  $J$  by  $I/A$ , where  $A$  is the effective emission area, and  $F$  by  $\beta V$ , where  $\beta$  is the geometrically determined field factor, we can rewrite Eq. (3) into the logarithmic form of Fowler-Nordheim plot (F-N plot)

$$\ln\left(\frac{I}{V^2}\right) = \ln\left(A \cdot 1.54 \times 10^{-6} \frac{\beta^2}{\phi}\right) - 6.83 \times 10^7 \frac{\phi^{3/2}}{\beta} \cdot \frac{1}{V}. \quad (4)$$

Figure 2(c) shows the F-N plot which exhibits a good linearity with correlation coefficient above 0.996 and the slope  $k$  is  $4865 \text{ eV}^{3/2} \text{ cm}$ . Since it is difficult to know the field factor  $\beta$  which can be from  $1/(5r)$  to  $1/(100r)$  depending on the emitter geometry,<sup>22,23</sup> here, we choose the approximation proposed by Charbonnier and Martin to express the F-N formula as<sup>24</sup>

$$J = 1.14 \times 10^9 \phi^2 e^{10.4/\sqrt{\phi}} \frac{e^{-2.3m/V}}{(m/V)^2}, \quad (5)$$

where  $m = -\frac{d[\log_{10}(I/V^2)]}{d(1/V)} = -\frac{1}{\ln 10} \cdot \frac{d[\ln(I/V^2)]}{d(1/V)} = -\frac{1}{\ln 10} k$ . The value of  $m$  is 2113 for our emitter. From the FIM image shown in Figure 1(b) and the SEM image shown in Figure 1(c), we can approximately take the tip as a hemisphere with a radius of 15.4 nm, which is the average value of the radius at the corner and at the center, and the total area of the {111} facet as about 15% of the whole tip surface area. This gives rise to an emitting area of about  $2.24 \times 10^{-12} \text{ cm}^2$  and thus,  $J = \frac{I}{2.24 \times 10^{-12}} \text{ A}/\text{cm}^2$ . Figure 2(d) shows the linear relationship between  $J$  and  $1.14 \times 10^9 e^{-2.3m/V}/(m/V)^2$  according to Eq. (5) and the slope which equals to  $\phi^2 e^{10.4/\sqrt{\phi}}$  is 3307. From the above data, the work function is obtained to be  $\phi = 3.4 \text{ eV}$  for our emitter. This is in good agreement with the value of 3.3 eV reported by Mackie *et al.* of the work function of HfC measured from field emission spectroscopic experiment.<sup>25</sup>

In conclusion, a single HfC nanowire field emitter has been assembled and the emitter tip was cleaned with low

temperature field evaporation. Stable field emission patterns have been obtained and a low work function of 3.4 eV of the {111} crystal surface has been deduced. Comparing with an HfC needle emitter, the localization of electron emission to the HfC {111} nano-facets promises a highly efficient electron emitter with high brightness and low energy spread, making the HfC nanowire emitter a potential point electron source for the field emission electron microscopes and its arrayed structure an excellent candidate for large area Spindt field emitters,<sup>26</sup> which now have been able to afford a current density as high as  $17 \text{ A}/\text{cm}^2$ .<sup>27</sup>

This work was partially supported by the Development of System and Technology for Advanced Measurement and Analysis, Japan Science and Technology Corporation (JST), and the Nanotechnology Network Project of the Ministry of Education, Culture, Sports, and Technology (MEXT), Japan.

<sup>1</sup>L. E. Toth, *Transitional Metal Carbide and Nitrides* (Academic, New York, 1971).

<sup>2</sup>E. K. Storms, *The Refractory Carbide* (Academic, New York, 1964).

<sup>3</sup>K. J. Kagarice, G. G. Magera, S. D. Pollard, and W. A. Mackie, *J. Vac. Technol. B*, **26**, 868 (2008).

<sup>4</sup>H. Adachi, *Scan Electron Microsc.* **2**, 473 (1985).

<sup>5</sup>H. Zhang, H. Zhang, Q. Zhang, J. Tang, and L.-C. Qin, *J. Am. Chem. Soc.* **127**, 2862 (2005).

<sup>6</sup>H. Zhang, Q. Zhang, J. Tang, and L.-C. Qin, *J. Am. Chem. Soc.* **127**, 8002 (2005).

<sup>7</sup>H. Zhang, Q. Zhang, G. Zhao, J. Tang, O. Zhou, and L.-C. Qin, *J. Am. Chem. Soc.* **127**, 13120 (2005).

<sup>8</sup>H. Zhang, J. Tang, Q. Zhang, G. Zhao, G. Yang, J. Zhang, O. Zhou, and L.-C. Qin, *Adv. Mater.* **18**, 87 (2006).

<sup>9</sup>G. Zhao, J. Zhang, Q. Zhang, H. Zhang, O. Zhou, L.-C. Qin, and J. Tang, *Appl. Phys. Lett.* **89**, 193113 (2006).

<sup>10</sup>G. Zhao, Q. Zhang, H. Zhang, G. Yang, O. Zhou, L.-C. Qin, and J. Tang, *Appl. Phys. Lett.* **89**, 263113 (2006).

<sup>11</sup>H. Zhang, J. Tang, L. Zhang, B. An, and L.-C. Qin, *Appl. Phys. Lett.* **92**, 173121 (2008).

<sup>12</sup>H. Zhang, J. Tang, J. Yuan, J. Ma, N. Shinya, K. Nakajima, H. Murakami, T. Ohkubo, and L.-C. Qin, *Nano Lett.* **10**, 3539 (2010).

<sup>13</sup>M. Futamoto, I. Yuito, U. Kawabe, O. Nishikawa, Y. Tsunashima, and Y. Hara, *Surf. Sci.* **120**, 90 (1982).

<sup>14</sup>H. Adachi, K. Fujii, S. Zaima, Y. Shibata, C. Oshima, S. Otani, and Y. Ishizawa, *Appl. Phys. Lett.* **43**, 702 (1983).

<sup>15</sup>E. W. Müller, *Science* **149**, 591 (1965).

<sup>16</sup>P. D. Prabhawalkark, V. S. Raghunathan, and S. Ranganathan, *Surf. Sci.* **51**, 441 (1975).

<sup>17</sup>T. T. Tsong and E. W. Müller, *J. Appl. Phys.* **38**, 3531 (1967).

<sup>18</sup>E. W. Müller, in *Advances in Electronics and Electron Physics*, edited by L. Marton (Academic, New York, 1960), Vol. **13**, pp. 83–177.

<sup>19</sup>L. W. Swanson, M. A. Gesley, and P. R. Davis, *Surf. Sci.* **107**, 263 (1981).

<sup>20</sup>W. A. Mackie, J. L. Morrissey, C. H. Hinrichs, and P. R. Davis, *J. Vac. Sci. Technol. A* **10**, 2852 (1992).

<sup>21</sup>I. Brodie and C. A. Spindt, in *Advances in Electronics and Electron Physics*, edited by P. W. Hawkes (Academic, San Diego, 1992), Vol. **83**, pp. 91–95.

<sup>22</sup>R. Gomer, *Field Emission and Field Ionization* (Harvard University Press, Cambridge, Massachusetts, 1961).

<sup>23</sup>C. J. Edgcombe and U. Valdrè, in *Proceedings of the International Centennial Symposium on the Electron*, edited by A. Kirkland and P. D. Brown (IDM Communication, London, 1997), pp. 318–325.

<sup>24</sup>F. M. Charbonnier and E. E. Martin, *J. Appl. Phys.* **33**, 1897 (1962).

<sup>25</sup>W. A. Mackie, L. A. Southall, T. Xie, G. L. Cabe, F. M. Charbonnier, and P. H. McClelland, *J. Vac. Sci. Technol. B* **21**, 1574 (2003).

<sup>26</sup>C. A. Spindt, *J. Appl. Phys.* **39**, 3504 (1968).

<sup>27</sup>F. G. Tarntair, L. C. Chen, S. L. Wei, W. K. Hong, K. H. Chen, and H. C. Cheng, *J. Vac. Sci. Technol. B* **18**, 1207 (2000).